Molecular Vision 2021; 27:354-364 <http://www.molvis.org/molvis/v27/354>
Received 1 July 2020 | Accepted 18 May 2021 | Published 20 May 2021

Piezo2 downregulation via the Cre-lox system affects aqueous humor dynamics in mice

Jingwang Fang,[1] Fei Hou,[1] Shen Wu,[2] Yani Liu,[1] Linna Wang,[3] Jingxue Zhang,[2] Ningli Wang,[2] Kewei Wang,[1,4] Wei Zhu[1,5]

[1]Department of Pharmacology, School of Pharmacy, Qingdao University, Qingdao, China; [2]Beijing Institute of Ophthalmology, Beijing Tongren Hospital Eye Center, Beijing, China; [3]Qingdao Haier Biotech Co. Ltd, Qingdao, China; [4]Institute of Innovative Drugs, Qingdao University, Qingdao, China; [5]Advanced Innovation Center for Big Data-Based Precision Medicine, Beijing University of Aeronautics and Astronautics-Capital Medical University, Beijing, China

Purpose: Proper aqueous humor (AH) dynamics is crucial for maintaining the intraocular pressure (IOP) in the eye. This study aims to investigate the function of Piezo2, a newly discovered mechanosensitive ion channel, in regulating AH dynamics.

Methods: Immunohistochemistry (IHC) analysis and western blotting were performed to detect Piezo2 expression. The Cre-lox system was applied to create a conditional knockout model of Piezo2. IOP and aqueous humor outflow facility in live animals were recorded with a Tonometer and a syringe-pump system for up to 2 weeks.

Results: We first detected Piezo2 with robust expression in the human trabecular meshwork (TM), Schlemm's canal (SC), the ciliary body's epithelium, and ciliary muscle. In addition, we found Piezo2 in human retinal ganglion cells (RGCs) and astrocytes in the optic nerve head (ONH). Through the Cre-lox system, Piezo2 can be successfully downregulated in mouse iridocorneal angle tissues. However, Piezo2 downregulation cannot significantly influence the IOP and outflow facility through the conventional pathway. Instead, we observed an effect of downregulated Piezo2 on decreasing the intercept in the flow rate versus pressure plot. According to the Goldmann equation, Piezo2 may function in regulating unconventional outflow, AH production, and episcleral venous pressure.

Conclusions: These findings, for the first time, demonstrate that Piezo2 acts as an essential mechanosensor in maintaining the proper aqueous humor dynamics in the eye.

Stable intraocular pressure (IOP), primarily depending on the balance of an equal rate between the production and drainage of aqueous humor (AH), is crucial for the maintenance of normal vision [1]. AH is secreted by the ciliary body and flows through the pupil to enter the anterior chamber [2]. AH drainage from the anterior chamber mainly depends on the conventional outflow pathway, especially in glaucomatous eyes [3,4]. In addition to the conventional outflow, a fraction of AH outflow is through an alternative AH drainage pathway called unconventional outflow [5,6]. Disruption of the balance of AH inflow and outflow can cause a sustained elevation of IOP or hypotony, leading to neuronal injury and abnormal vision [7,8].

Several mechanical responders have been reported to regulate AH dynamics, such as nitric oxide (NO) signal [9,10], caveolin [11], and a mechanosensitive ion channel [12]. Mechanosensitive ion channels are one type that can sense mechanical stimuli and transduce mechanical signals rapidly [13]. Several mechanosensitive ion channels have been discovered in regulating AH outflow, such as TREK-1 [14] and TRPV4 [15]. A novel class of mechanosensitive channel, Piezo2, was discovered recently with essential roles in mechanosensory. In addition to responsibility for gentle touch sensation in the skin [16-18], and the signal conversion of touch to itch [19], Piezo2 has been reported to maintain balance and coordination [20,21], airway stretch, and lung inflation [22]. However, the function of Piezo2 in the regulation of AH dynamics is still unknown.

This study aimed to investigate the expression of Piezo2 in the ocular tissues and its roles in AH dynamics. Through the Cre-lox system, Piezo2 expression in mouse iridocorneal tissues was downregulated, and its function in regulating AH dynamics was directly measured and estimated.

METHODS

Human materials: Tissues from three healthy 60- to 70-year-old Caucasian adults without any systemic disease were collected from the Lion Eye Bank of the United States (Iowa, IA). The dissected tissues were immediately fixed in 4% paraformaldehyde (Thermo, Waltham, MA), infiltrated in sucrose solution (Sigma, St. Louis, MO), and embedded in optimum cutting temperature (OCT) compound (Sakura,

Correspondence to: Wei Zhu, Department of Pharmacology, Qingdao University, 38 Dengzhou Rd., Qingdao, Shandong 266021, China; Phone: +86(0532)82991202; FAX: +86(0532)83801449; email: wzhu@qdu.edu.cn

Tokyo, Japan). The protocol for collecting human tissues was approved by the Eye Bank Association of America.

HTM culture: As previously described [23], human TM (HTM) cells were isolated from three other healthy 60- to 70-year-old human donors obtained from Lion Eye Bank of United States. Briefly, the TM was dissected and treated with collagenase A (4mg/ml) in DPBS for 2 hours. After centrifugation, the pellet containing the cells was maintained in Medium 199 (Gibco, Frederick, MD), containing 20% fetal bovine serum (FBS; Gibco), 90 μg/ml porcine heparin (Sigma-Aldrich), 20 U/ml endothelial cell growth supplement (Sigma-Aldrich) and 1.7 mM L-glutamine (Sigma-Aldrich). Isolated HTM cells were characterized by detecting the robustly expressed TM biomarkers and dexamethasone-induced myocilin expression, and used for identifying Piezo2 expression by Western blot. Isolated HTM cells were characterized by detecting the robustly expressed TM biomarkers and dexamethasone-induced myocilin expression, cultured in TM cell growth medium comprised 199E medium (Gibco, Frederick, MD) containing 20% fetal bovine serum (FBS; Gibco), 90 μg/ml porcine heparin (Sigma-Aldrich), 20 U/ml endothelial cell growth supplement (Sigma-Aldrich), and 1.7 mM L-glutamine (Sigma-Aldrich), and used for identifying Piezo2 expression with western blotting. The collection protocol for human TM cells were approved by the Eye Bank Association of America. This study adhered to the tenets of the Declaration of Helsinki and the ARVO statement for the Use of Human Subjects.

Mice: Homozygous Piezo2$^{fl/fl}$ mice on a background of C57BL/6J were obtained from Tsinghua University (Beijing, China). They were bred under a standard housing condition at Qingdao University Medical Center (Qingdao, China) with a 12 h:12 h light-dark cycle, controlled humidity of 45%–55%, and a room temperature of 22–24 °C. Two-month-old male homozygous Piezo2$^{fl/fl}$ mice and age-matched male C57BL/6J mice purchased from Beijing Vital River Laboratory Animal Technology Co, Ltd (Beijing, China) were used for the IOP and outflow facility measurements. All experimental procedures that were approved by Qingdao University Medical Center conformed to institutional guidelines for laboratory animal care and use. The study adhered to the ARVO Statement for the Use of Animals in Research.

Immunohistochemistry study: The embedded tissues were sliced into 10-μm-thick sections with the Cryostat system (Leica, Nussloch, Germany). The sections were rinsed in Dulbecco's PBS (1×; 0.9 mM $CaCl_2$, 0.5mM $MgCl_2$, 138 mM NaCl, 2.7 mM KCl, 8 mM Na_2HPO_4, 1.5 mM KH_2PO_4, pH 7.0-7.2; DPBS) for 5 min and incubated in the blocking solution (DPBS with 1% bovine serum albumin, BSA; Sigma, St. Louis, MO) for 1 h. After incubation with the diluted primary antibodies (1:100) overnight at 4 °C and rinsing with DPBS three times, the sections were then incubated with the corresponding secondary antibodies (1:200) at room temperature for 1 h. The tissue nuclei were stained with 4′,6-diamidino-2-phenylindole (DAPI; Santa Cruz, Dallas, TX). The stained sections were mounted using Neutral Balsam (Solarbio, Beijing, China) and imaged with confocal microscopy (Nikon, Tokyo, Japan). The imaged TM tissues were zoned into three regions, uveal meshwork, corneoscleral meshwork, and the juxtacanalicular tissue (JCT) based on previous publications [24]. The nuclei and Piezo2-positive cells in each region were counted automatically with TissueQuest software (TissueGnostics GmbH, Vienna, Austria). Data from six sections of each individual were averaged and used for statistical analysis (n = 3). The primary antibodies included rabbit polyclonal antibody anti-Piezo2 (NBP1–78624, Novus, Littleton, CO), mouse polyclonal antibodies anti-Collagen IV (ab6311) and GFAP (ab10062, Abcam, Cambridge, MA), and mouse monoclonal antibody anti-SNCG (MAB5745, Novus). The secondary antibodies included immunoglobulin G (IgG) Alexa Fluor® 488 goat anti-mouse IgG (Invitrogen, Carlsbad, CA) and IgG Alexa Fluor® 568 goat anti-rabbit IgG (Invitrogen). To eliminate non-specific staining, the tissue stained with the secondary antibodies was used as the negative control.

Western blotting: Proteins in mouse iridocorneal angles were extracted using radioimmunoprecipitation assay (RIPA) buffer supplemented with Halt™ Protease Inhibitor Cocktail (Thermo). Protein was quantified using the BSA Protein Reagent Kit (Thermo). Thirty microns of total protein were loaded on 5% sodium dodecyl sulfate (SDS)-acrylamide gel and separated with 10% SDS-acrylamide gel electrophoresis. The proteins were then transferred to a polyvinyl difluoride membrane (GE Healthcare, Boston, MA) using a Trans-blot Turbo Transfer System (Bio-Rad, Hercules, CA) under the condition of 200 mA for 90 min. The membranes were incubated with the blocking buffer at room temperature for 1 h and primary antibodies against Piezo2 (ab81327, Abcam) or β-actin (ab8226, Abcam). The membrane was further incubated with goat anti-rabbit IgG conjugated with horseradish peroxidase (HRP; Abcam). Immunoreactive bands were detected with enhanced chemiluminescence detection with SuperSignal West Pico PLUS Chemiluminescent Substrate (Thermo) in the Image Lab imaging system (Bio-Rad, Hercules, CA). Band intensities of Piezo2 were quantified with the Image Lab imaging system (Bio-Rad) and normalized to β-actin.

Preparation of adenovirus 5 (Ad5): The plasmids of pDC311 and pBHGlox E1, 3 Cre were cotransfected into human embryonic kidney (HEK)293 cells using LipoFilter™ transfection reagent (Hanbio, Shanghai, China) to generate the recombinant adenovirus 5. HEK293 cell line was authenticated using Short Tandem Repeat (STR) analysis (Vigene Biosciences, Jinan, China), as described in 2012 in ANSI Standard (ASN-0002) by the ATCC Standards Development Organization (SDO). Nineteen STR loci plus the gender determining locus, Amelogenin, was amplified using the commercially available EX20 Kit from AGCU. The cell line sample was processed using the ABI Prism® 3130 XL Genetic Analyzer. Data were analyzed using GeneMapper® ID v3.2 software (Applied Biosystems). Appropriate positive and negative controls were run and confirmed for each sample submitted. The STR analyses were presented in a Appendix 1. The propagated recombinant adenoviruses in HEK293 cells were purified. The titer of the virus determined with plaque assays was 1×10^{12} plaque formation unit (PFU)/ml. Adenoviruses harboring green fluorescent protein (GFP) and scrambled oligo were used as control. About 1×10^{8} PFU Ad5 carrying CMV-Con-GFP or CMV-Cre-GFP were injected into the anterior chambers of homozygous Piezo2$^{fl/fl}$ mice.

Experimental design: The Piezo2$^{fl/fl}$ mice were divided into three groups, including control mice injected with the 0.9% saline (n = 21) and mice receiving Ad5-Con (n = 34) or Ad5-Cre virus (n = 45). IOP was tracked weekly until the second week after injection. One week after injection, some of the control mice (n = 6) and the mice receiving Ad5-Con (n = 14) or Ad5-Cre virus (n = 15) were selected for the invasive outflow facility measurement. In the second week of injection, the remaining control mice (n = 7) and Ad5-Con- (n = 16) and Ad5-Cre- (n = 18) injected mice were further analyzed.

Intracameral Injection: Mice were sedated using 8% chloral hydrate (0.125 ml/20 g) and kept on a heating blanket (37 °C) until recovery. About 1×10^{8} PFU Ad5 in 1.5 µl saline was delivered slowly into the anterior chamber of the eye using a 10 µl Hamilton syringe (Hamilton, Reno, NV) with 30-gauge 1/2-inch length sterile needles (Becton Dickenson, Franklin Lakes, NJ) [25,26].

IOP measurement: Mice were anesthetized with 2.5% isoflurane (wt/vol) plus 80% (vol/vol) oxygen in a sealed chamber for 5 min and further anesthetized for 1 min by using the mask. IOP was measured using a rebound tonometer (TonoLab, Helsinki, Finland), as described previously [27]. All measurements were taken between 9 and 11 AM.

Outflow facility measurement: As described previously [27], the mice were anesthetized with 8% chloral hydrate (0.125 ml/20 g) and kept on a heating blanket (37 °C) during the measurement. The outflow facility was measured with a syringe-pump system. The eyes were cannulated with a 30-gauge 1/2-inch length sterile needles (Becton Dickenson), and 0.9% saline was pumped into the eye through a 100 µl Hamilton syringe, which was mounted on a computer-controlled pump (AL-1000, World Precision Instruments, Sarasota, FL). The ocular pressure transduced with a flow-through pressure sensor (Icu Medical, San Clemente, CA) was recorded in Hemo Lab software (Stauss Scientific, Iowa, IA). Three sequential pressure steps of 15, 25, and 35 mmHg were applied to the eyes, while the flow rates (µl/min) were recorded for 15 min. The averaged flow rates and the pressures at each step were used to generate a flow rate-pressure plot. The line fitting to a linear regression was added in the data set, the slope of which was considered a conventional outflow facility (µl/min/mmHg).

Intercept calculation: According to the modified Goldmann equation:

$$Q_{in} + Q_{pump} = C\ (IOP - P_{ev}) + Q_{un}, \quad (1)$$

where Q_{in} is the AH production rate, Q_{pump} is the pumping rate, IOP is the intraocular pressure, P_{ev} is the pressure of the episcleral vessel, and C is the outflow facility through the conventional outflow. Q_{un} is the flow rate from unconventional outflow [28]. When the pressure is zero, the modified equation becomes:

$$Q_{pump} = Q_{un} - Q_{in} - C \times P_{ev}, \quad (2)$$

where the intercept, Q_{pump}, is reflected by unconventional outflow, inflow rate, conventional outflow, and episcleral venous pressure.

Statistical analysis: One-way analysis of variance (ANOVA) was applied to analyze the immunohistochemistry (IHC) and western blotting results. A two-tailed *t* test and a normality test were used for statistical analyses in the animal study. P values of less than 0.05 were considered statistically significant. Data in this study were expressed as the mean ± standard error of the mean (SEM).

RESULTS

Robust expression of Piezo2 in the human trabecular meshwork and Schlemm's canal: Representative images with costaining of Piezo2 (red) and Collagen IV (green) for labeling the TM are shown in Figure 1. The IHC results demonstrated that Piezo2 was robustly expressed in the TM and SC tissues of three human donors (Figure 1A). According to the TM histological structure [2], Piezo2-positive cell fractions in three TM regions were further analyzed. Interestingly, 73.0% ± 19.1% cells in the uveal meshwork were detected to express

Piezo2, whereas the fractions were only 39.9% ± 6.20% cells in the corneoscleral meshwork and 22.3% ± 7.60% cells in the JCT region (n = 3; Figure 1B). The fluorescent intensity of Piezo2 in the three TM regions was the same (Figure 1B). The existence of Piezo2 in the TM was further confirmed through detecting its expression in HTM cells cultured in vitro with western blotting (Figure 1C). In addition to the TM, Piezo2 was expressed in the Schlemm's canal endothelial cells (Figure 1A).

Expression of Piezo2 in human non-pigmented epithelial cells and ciliary muscle: We further determined the expression of Piezo2 in human tissues responsible for AH production and unconventional outflow. The IHC results revealed that Piezo2 was expressed in non-pigmented epithelial (NPE) and pigmented epithelial (PE) cells, mainly in NPE cells and ciliary muscle (Figure 1D).

Localization of Piezo2 in the human retina and optic nerve: Piezo2 expression was also detected in the nerve fiber layer (NFL), ganglion cell layer (GCL), inner nuclear layer (INL), and outer nuclear layer (ONL) with positive fractions of 0.80, 0.54, 0.32, and 0.65, respectively (Figure 2A–C). Piezo2 was observed with robust expression in the lamina cribrosa region (Figure 2D). These results suggested that Piezo2 was expressed by multiple neural cells in the retina and optic nerve. Co-IHC analyses with Piezo2 (red) and glial fibrillary acidic proteins (GFAP, green) for labeling astrocytes or synuclein gamma (SNCG, green) for labeling RGCs indicated that Piezo2 could be expressed in RGCs and astrocytes (Figure 2).

Piezo2 expression in mouse iridocorneal tissues: The expression of Piezo2 in mouse iridocorneal tissues was investigated with western blotting and IHC. Western blotting results indicated that the expression of Piezo2 was 0.47-fold compared to Piezo2 expression in the dorsal root ganglia

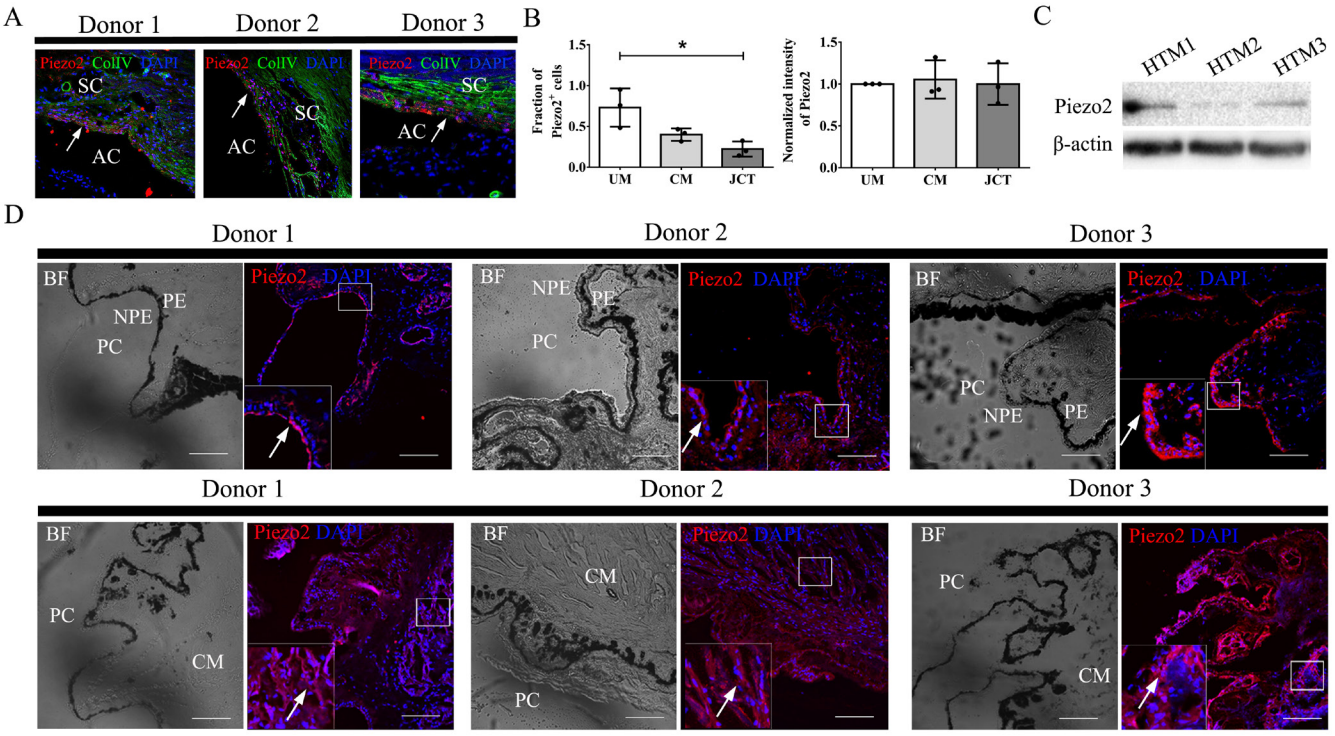

Figure 1. Piezo2 expression in human iridocorneal angle tissues. **A**: Piezo2 (red) was expressed in the TM labeled with Collagen IV (ColIV) antibody (green), and the SC endothelial cells of three human donors. The nuclei were stained with 4′,6-diamidino-2-phenylindole (DAPI in blue. **B**: Piezo2-positive cell fraction were 73.0% ± 19.1%, 39.9% ± 6.20%, and 22.3% ± 7.60% in the UM, CM, and JCT (n = 3). A statistically significantly higher Piezo2-positive cell number was detected in the UM than in the JCT and the CM (p = 0.01, n = 3). No statistically significant difference in fluorescence intensity was observed in different regions of the TM (n = 3). * p<0.05 with one-way analysis of variance (ANOVA). **C**: Piezo2 expression was detected in HTM cells cultured in vitro with western blotting. β-actin was used as the reference protein. **D**: Top panel: Piezo2 (red) were detected in NPE and PE cells, especially in NPE cells. Bottom panel: Piezo2 (red) was detected in ciliary muscle robustly. In-focus images are shown in higher magnification on the bottom left. Scale bar: 100 µm. TM: trabecular meshwork, SC: Schlemm's canal, CB: ciliary body, UM: uveal meshwork, CM: corneoscleral meshwork, JCT: juxtacanalicular tissue, AC: anterior chamber, PC: posterior chamber, NPE: non-pigmented epithelium cells, PE: pigmented epithelium cells, CM: ciliary muscle.

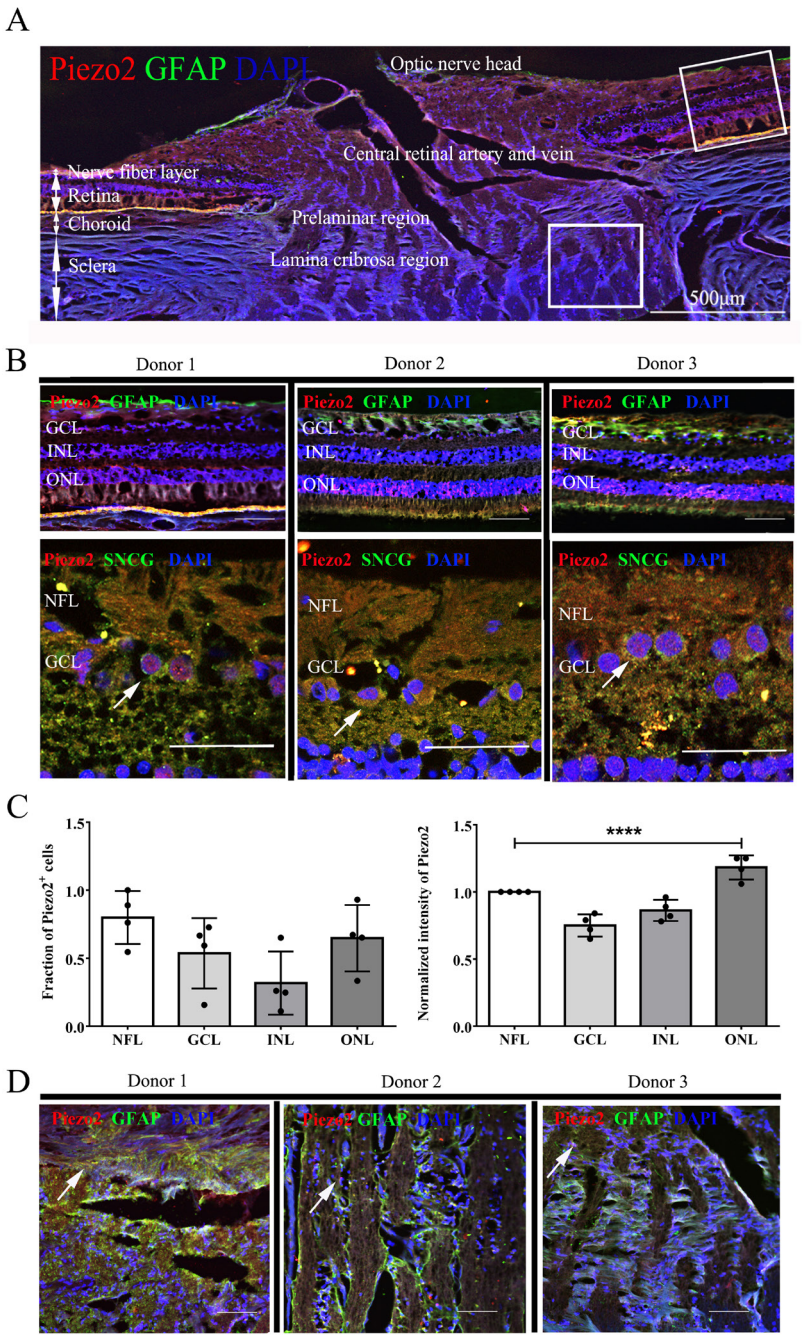

Figure 2. Piezo2 expression in neural cells of human retina and optic nerve. **A**: An image of the human retina and optic nerve head with Piezo2 immunofluorescence (red) and 4′,6-diamidino-2-phenylindole (DAPI) nuclei (blue) is presented. The retinal (**B**) and ONH (**D**) tissues in white frames are shown in high magnification. **B**: Piezo2 (red) was detected in the NFL, GCL, INL, and ONL. Colabeling analysis with Piezo2 (red) and SNCG (green) or GFAP (green) antibodies indicates retinal ganglion cells (RGCs) and astrocytes could express Piezo2. **C**: Piezo2-positive cell fractions were 0.80, 0.54, 0.32, and 0.65 in the NFL, GCL, INL, and ONL (n = 3). Statistically significantly higher expression of Piezo2 was observed in the ONL ($p<0.0001$, n = 3). ****$p<0.0001$ with one-way analysis of variance (ANOVA). **D**: Co-IHC analysis with Piezo2 (red) and GFAP (green) antibodies indicated that astrocytes in the ONH express Piezo2. The nuclei were stained with 4′,6-diamidino-2-phenylindole (DAPI) in blue. Scale bar: 50 μm. NFL: nerve fiber layer, GCL: ganglion cell layer, INL: inner nuclear layer, ONL: outer nuclear layer, ONH: human optic nerve head, SNCG: synuclein gamma, GFAP: glial fibrillary acidic protein.

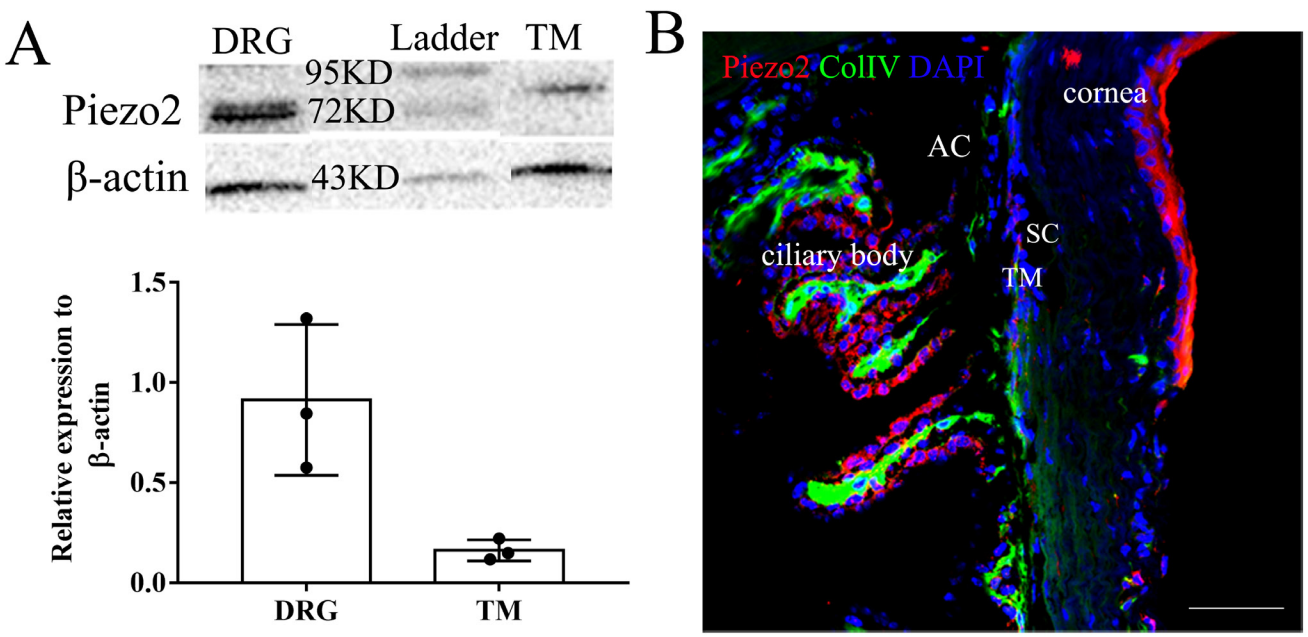

Figure 3. Expression of Piezo2 in mouse iridocorneal angle tissues. **A**: Expression of Piezo2 in iridocorneal angle tissues of Piezo2$^{fl/fl}$ mice (n = 5) was determined with western blotting and normalized to the amount of β-actin. Piezo2 was abundant in the mouse iridocorneal angle tissues compared to Piezo2 expression in the dorsal root ganglia (DRG). Normalized band intensities of Piezo2 in the DRG and the trabecular meshwork (TM) are displayed. **B**: Type IV collagen in mouse iridocorneal angle tissues is highlighted with the Collagen IV (ColIV) antibody in green. Piezo2 (red) expression was detected in the TM, the ciliary body's epithelium, ciliary muscle, and cornea. The nuclei were stained with 4′,6-diamidino-2-phenylindole (DAPI) in blue. Scale bar: 100 µm.

(DRG), suggesting that the Piezo2 channel is abundant in mouse iridocorneal tissues (Figure 3A). Furthermore, the IHC study revealed that Piezo2 was expressed throughout the TM, ciliary body's epithelium, ciliary muscle, and cornea (Figure 3B).

Piezo2 downregulation in mouse iridocorneal tissues via the Cre-lox system: The Cre-lox system was applied to create a conditional knockout mouse model of Piezo2. Intracameral injection with Ad5-Con or Cre was performed in the Piezo2$^{fl/fl}$ mouse, and Piezo2 expression was determined with western blotting and IHC. Compared to the Ad5-Con group, Piezo2 expression was decreased by approximately 21.4% and 35.1% at the first and second weeks after the Ad5-Cre injection ($p = 0.04$; Figure 4A). The IHC results revealed that the Piezo2 expression regulated through the Cre-lox system was statistically significantly decreased in the TM, ciliary body, and ciliary muscle (Figure 4B).

Piezo2 function in the regulation of aqueous humor dynamics: The IOP was measured weekly in three groups of mice, the Piezo2$^{fl/fl}$ mice and the Piezo2$^{fl/fl}$ mice receiving Ad5-Con or Ad5-Cre. Compared to the Ad5-Con treated Piezo2$^{fl/fl}$ mice, no statistically significant change in the IOP can be observed in the Piezo2$^{fl/fl}$ mice receiving Ad5-Cre whether in the first or second week of injection (Figure 5A). In the second week of injection, the averaged outflow facility in the Piezo2$^{fl/fl}$ mice was 0.0158±0.0060 µl/min/mmHg (Figure 5B). Compared to the Ad5-Con group (0.0139±0.0080 µl/min/mmHg), the injection of Ad5-Cre for 2 weeks mildly increased the outflow facility to 0.0176±0.0100 µl/min/mmHg, but no statistical significance was observed ($p = 0.22$; Figure 5B). These results suggested that Piezo2 exhibits a negligible role in the conventional outflow of aqueous humor under the physiologic condition.

In the flow rate-pressure plot, the intercept of the line was 0.21±0.17 µl/min in the eyes of the Piezo2$^{fl/fl}$ mice in the second week of injection (Figure 5C). Compared to the Ad5-Con group (0.20±0.11 µl/min), the injection of Ad5-Cre for 2 weeks statistically significantly decreased the intercept to 0.09±0.17 µl/min ($p = 0.04$; Figure 5C). According to the Goldmann equation, these data indicated that Piezo2 might function in unconventional outflow, AH production, or episcleral venous pressure, or all.

Discussion: The trabecular meshwork cells responsible for the conventional AH outflow are a group of mechanosensitive

cells [29]. Previous investigations have demonstrated a new type of ion channel, Piezo, in the TM [12,30]. In this study, the expression pattern of Piezo2 was further analyzed with robust expression in the uveal meshwork and a mild expression in

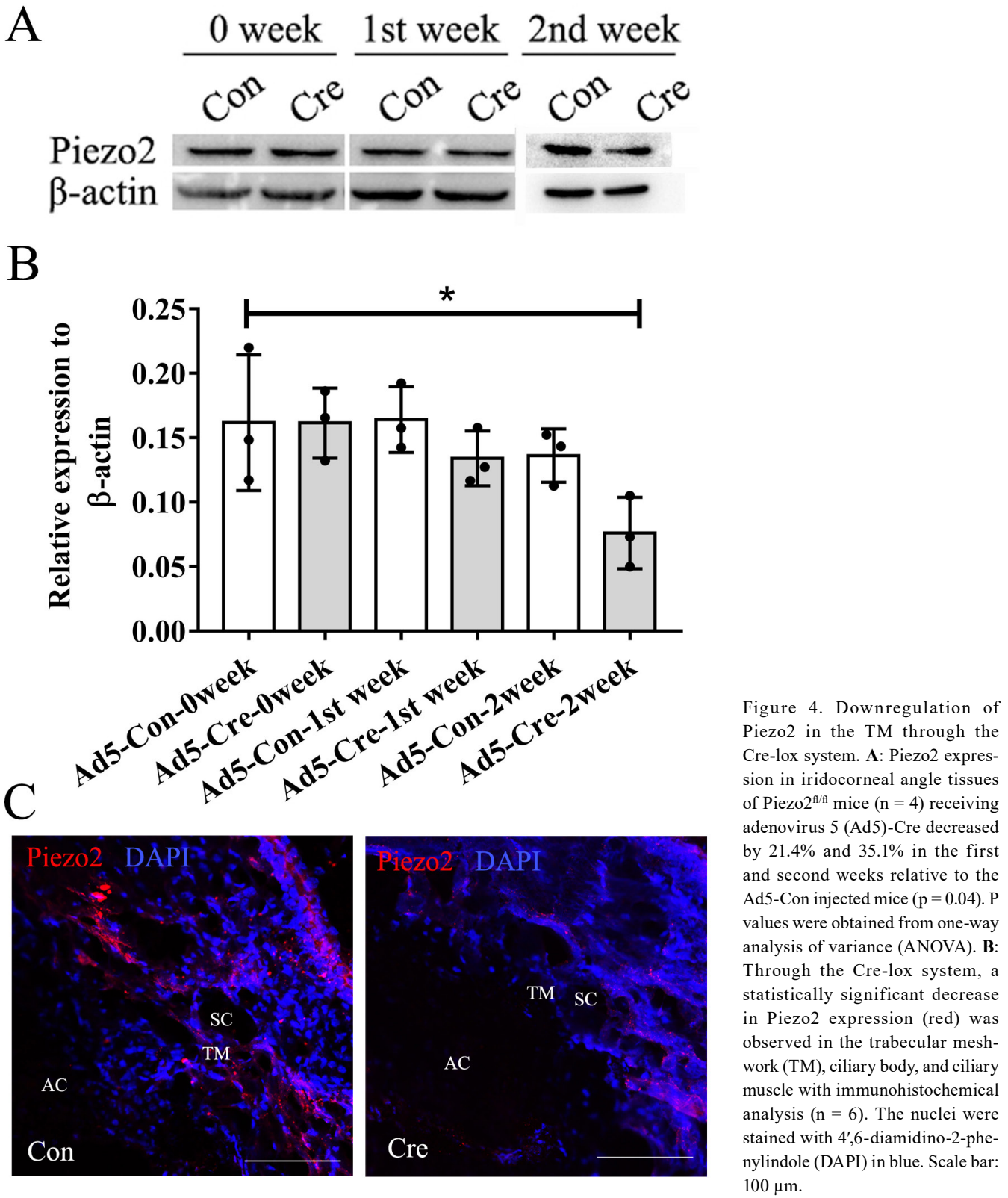

Figure 4. Downregulation of Piezo2 in the TM through the Cre-lox system. **A**: Piezo2 expression in iridocorneal angle tissues of Piezo2$^{fl/fl}$ mice (n = 4) receiving adenovirus 5 (Ad5)-Cre decreased by 21.4% and 35.1% in the first and second weeks relative to the Ad5-Con injected mice (p = 0.04). P values were obtained from one-way analysis of variance (ANOVA). **B**: Through the Cre-lox system, a statistically significant decrease in Piezo2 expression (red) was observed in the trabecular meshwork (TM), ciliary body, and ciliary muscle with immunohistochemical analysis (n = 6). The nuclei were stained with 4′,6-diamidino-2-phenylindole (DAPI) in blue. Scale bar: 100 µm.

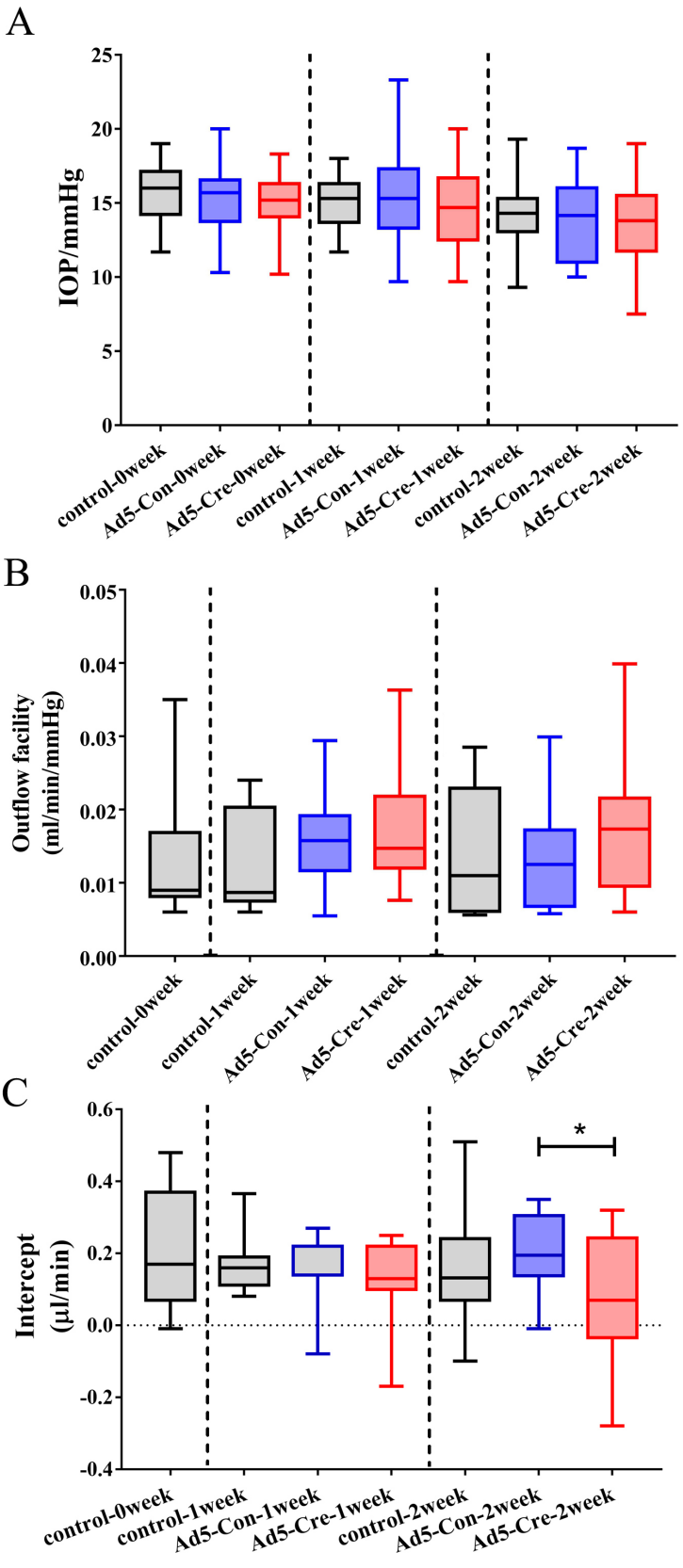

Figure 5. Piezo2 function in regulating aqueous humor dynamics. A: No statistically significant change in the intraocular pressure (IOP) was detected in the Piezo2$^{fl/fl}$ mice receiving adenovirus 5 (Ad5)-Cre (13.4±2.90 mmHg, n = 45) compared to mice receiving Ad5-Con (13.9±2.70 mmHg, n = 34) during the first 2 weeks of injection. **B**: At the second week of injection, the outflow facility in mice receiving Ad5-Cre (0.0176±0.0100 µl/min/mmHg, n = 18) showed no statistically significant difference compared to the facility in mice receiving Ad5-Con (0.0139±0.0080 µl/min/mmHg, n = 16, p = 0.22). **C**: Two weeks after injection, the intercept of the linear regression line in the flow rate-pressure plot was decreased dramatically in the Piezo2$^{fl/fl}$ mice receiving Ad5-Cre (0.09±0.17 µl/min, n = 18) compared to the Ad5-Con injected mice (0.20±0.11 µl/min, n = 14, p = 0.04). *p<0.05, p values were obtained from a two-tailed *t* test.

the corneoscleral meshwork and JCT (Figure 1). It might be the reason for the different functions of cells in different TM regions. For example, cells in the uveal meshwork exhibit strong phagocytic capability [24], whereas cells in the JCT show a strong ability for extracellular matrix (ECM) turnover [31]. Schlemm's canal endothelial cells beneath the TM are another cell type that can efficiently regulate the conventional outflow [32]. The outflow resistance generated by these cells mainly depends on the ability of pore formation [33]. Pores in SC endothelial cells have been detected to be formed rapidly with mechanical forces [34]. In the present study, expression of Piezo2 was found in SC endothelial cells (Figure 1). As a type of mechanical sensor to respond stimuli in microseconds [35], Piezo2 holds the potential for rapid pore formation in SC endothelial cells.

These IHC observations suggested potential roles for Piezo2 in regulating the conventional outflow of aqueous humor (Figure 3). However, Piezo2 downregulation through the Cre-lox system cannot statistically significantly change conventional outflow (Figure 4 and Figure 5). A reason might be that Piezo2 downregulation cannot influence the TM and SC function under the physiologic condition. Another possibility might be that some mechanical responders in the TM and SC tissues other than Piezo2 play a more considerable role in the conventional outflow, such as TRPV4 and TREK1 [14,15].

Interestingly, a statistically significant decrease in the intercept in the flow rate-pressure plot was detected in the Ad5-Cre-treated Piezo2$^{fl/fl}$ mice (Figure 5). The intercept value is reflected by the unconventional outflow, AH production, and episcleral venous pressure (Equation 2). Compared to the Piezo2 expression in the TM and SC, Piezo2 exhibits relatively higher expression in the ciliary muscle and non-pigmented epithelial cells (Figure 1), suggesting a potential role regulating the unconventional outflow and AH secretion. The unconventional pathway contributes approximately 5%–24% of the entire outflow under the physiologic condition and holds more critical roles when there are some obstacles in the conventional outflow pathway. The ciliary muscle is considered critical in controlling the outflow from this pathway [36]. Some previous studies revealed that Piezo2 can function importantly in the development of skeletal muscles [37]. Mutations in the *Piezo2* gene are associated with numerous muscle-related diseases, such as arthrogryposis [38], scoliosis [37], and proprioception defects [20], neonatal respiratory insufficiency [22], and muscle weakness [39]. Another possible reason for the reduced intercept is that Piezo2 influences AH secretion. Previous investigations indicated that Piezo2 functions in the gastrointestinal tract to convert forces into serotonin release [40,41]. It is critical for normal epithelial fluid secretion and gastrointestinal motility. Our next study aims to investigate the real effect of Piezo2 on the unconventional outflow and AH secretion.

A recent study also suggested that Piezo1 can function in regulating neurite outgrowth of RGCs [42]. In the present study, Piezo2 was found in certain types of neural cells, such as RGCs and astrocytes (Figure 2). These findings suggested a potential role of Piezo2 in the regulation of the growth and function of neural cells in the retina and the optic nerve.

In summary, Piezo2 is robustly expressed in the ocular tissues related to aqueous humor dynamics, including the trabecular meshwork, Schlemm's canal endothelial cells, ciliary muscle, and non-pigmented epithelial cells in the ciliary body. In a functional test, Piezo2 downregulation contributes to a statistically significant reduction of the intercept in the outflow rate versus pressure plot, but not the conventional outflow. It provides the potential for Piezo2 in regulating unconventional outflow, aqueous humor production, and episcleral venous pressure.

APPENDIX 1. STR ANALYSIS.

To access the data, click or select the words "Appendix 1."

ACKNOWLEDGMENTS

All authors do not have any conflicts of interest to declare. We thank Prof. Markus H. Kuehn at the University of Iowa, USA for providing human materials, and Prof. Bailong Xiao at Tsinghua University for providing homozygous Piezo2$^{fl/fl}$ mice. This study was supported by National Natural Science Foundation of China 81870653, National Key Research and Development Program 2018YFA0109500, Shandong Province National Science Foundation ZR2017BH007, and Shandong Province Key Research and Development Program 2019GSF107075.

REFERENCES

1. Chandler PA. Progress in the treatment of glaucoma in my lifetime. Surv Ophthalmol 1977; 21:412-28. [PMID: 325672].
2. Goel M, Picciani RG, Lee RK, Bhattacharya SK. Aqueous humor dynamics: a review. Open Ophthalmol J 2010; 4:52-9. [PMID: 21293732].
3. Weinreb RN, Aung T, Medeiros FA. The pathophysiology and treatment of glaucoma: a review. JAMA 2014; 311:1901-11. [PMID: 24825645].
4. Fine BS. Structure of the trabecular meshwork and the canal of Schlemm. Trans Am Acad Ophthalmol Otolaryngol 1966; 70:777-90. [PMID: 5970714].

5. Lindsey JD, Weinreb RN. Identification of the mouse uveoscleral outflow pathway using fluorescent dextran. Invest Ophthalmol Vis Sci 2002; 43:2201-5. [PMID: 12091417].

6. Johnson M, McLaren JW, Overby DR. Unconventional aqueous humor outflow: A review. Exp Eye Res 2017; 158:94-111. [PMID: 26850315].

7. . The Advanced Glaucoma Intervention Study (AGIS). 7. The relationship between control of intraocular pressure and visual field deterioration.The AGIS Investigators. Am J Ophthalmol 2000; 130:429-40. [PMID: 11024415].

8. Buckingham BP, Inman DM, Lambert W, Oglesby E, Calkins DJ, Steele MR, Vetter ML, Marsh-Armstrong N, Horner PJ. Progressive ganglion cell degeneration precedes neuronal loss in a mouse model of glaucoma. J Neurosci 2008; 28:2735-44. [PMID: 18337403].

9. Wiederholt M, Sturm A, Lepple-Wienhues A. Relaxation of trabecular meshwork and ciliary muscle by release of nitric oxide. Invest Ophthalmol Vis Sci 1994; 35:2515-20. [PMID: 7512945].

10. Ellis DZ, Sharif NA, Dismuke WM. Endogenous regulation of human Schlemm's canal cell volume by nitric oxide signaling. Invest Ophthalmol Vis Sci 2010; 51:5817-24. [PMID: 20484594].

11. Elliott MH, Ashpole NE, Gu X, Herrnberger L, McClellan ME, Griffith GL, Reagan AM, Boyce TM, Tanito M, Tamm ER, Stamer WD. Caveolin-1 modulates intraocular pressure: implications for caveolae mechanoprotection in glaucoma. Sci Rep 2016; 6:37127-38. .

12. Tran VT, Ho PT, Cabrera L, Torres JE, Bhattacharya SK. Mechanotransduction channels of the trabecular meshwork. Curr Eye Res 2014; 39:291-303. [PMID: 24215462].

13. Ranade SS, Syeda R, Patapoutian A. Mechanically Activated Ion Channels. Neuron 2015; 87:1162-79. [PMID: 26402601].

14. Carreon TA, Castellanos A, Gasull X, Bhattacharya SK. Interaction of cochlin and mechanosensitive channel TREK-1 in trabecular meshwork cells influences the regulation of intraocular pressure. Sci Rep 2017; 7:452-62. .

15. Jo AO, Lakk M, Frye AM, Phuong TT, Redmon SN, Roberts R, Berkowitz BA, Yarishkin O, Krizaj D. Differential volume regulation and calcium signaling in two ciliary body cell types is subserved by TRPV4 channels. Proc Natl Acad Sci USA 2016; 113:3885-90. [PMID: 27006502].

16. Ikeda R, Cha M, Ling J, Jia Z, Coyle D, Gu JG. Merkel cells transduce and encode tactile stimuli to drive Abeta-afferent impulses. Cell 2014; 157:664-75. [PMID: 24746027].

17. Ranade SS, Woo SH, Dubin AE, Moshourab RA, Wetzel C, Petrus M, Mathur J, Begay V, Coste B, Mainquist J, Wilson AJ, Francisco AG, Reddy K, Qiu Z, Wood JN, Lewin GR, Patapoutian A. Piezo2 is the major transducer of mechanical forces for touch sensation in mice. Nature 2014; 516:121-5. [PMID: 25471886].

18. Woo SH, Ranade S, Weyer AD, Dubin AE, Baba Y, Qiu Z, Petrus M, Miyamoto T, Reddy K, Lumpkin EA, Stucky CL, Patapoutian A. Piezo2 is required for Merkel-cell mechanotransduction. Nature 2014; 509:622-6. [PMID: 24717433].

19. Feng J, Luo J. Piezo2 channel-Merkel cell signaling modulates the conversion of touch to itch. Science 2018; 360:530-3. .

20. Woo SH, Lukacs V, de Nooij JC, Zaytseva D, Criddle CR, Francisco A, Jessell TM, Wilkinson KA. Piezo2 is the principal mechanotransduction channel for proprioception. Nat Neurosci 2015; 18:1756-62. .

21. Florez-Paz D, Bali KK, Kuner R, Gomis A. A critical role for Piezo2 channels in the mechanotransduction of mouse proprioceptive neurons. Sci Rep 2016; 6:25923-31. .

22. Nonomura K, Woo SH, Chang RB, Gillich A, Qiu Z, Francisco AG, Ranade SS, Liberles SD, Patapoutian A. Piezo2 senses airway stretch and mediates lung inflation-induced apnoea. Nature 2017; 541:176-81. [PMID: 28002412].

23. Yu H, Miao Y, Chen W, Qi X, Yang X, Pan X, Wang K, Zhu W. Expressional and functional involvement of gap junctions in aqueous humor outflow into the ocular trabecular meshwork of the anterior chamber. Mol Vis 2019; 25:255-65. [PMID: 31205407].

24. Stamer WD, Clark AF. The many faces of the trabecular meshwork cell. Exp Eye Res 2017; 158:112-23. [PMID: 27443500].

25. Stout CE, Costantin JL, Naus CC, Charles AC. Intercellular calcium signaling in astrocytes via ATP release through connexin hemichannels. J Biol Chem 2002; 277:10482-8. [PMID: 11790776].

26. Adermark L, Lovinger DM. Electrophysiological properties and gap junction coupling of striatal astrocytes. Neurochem Int 2008; 52:1365-72. [PMID: 18396351].

27. Zhu W, Jain A, Gramlich OW, Tucker BA, Sheffield VC, Kuehn MH. Restoration of Aqueous Humor Outflow Following Transplantation of iPSC-Derived Trabecular Meshwork Cells in a Transgenic Mouse Model of Glaucoma. Invest Ophthalmol Vis Sci 2017; 58:2054-62. [PMID: 28384726].

28. Brubaker RF. Goldmann's equation and clinical measures of aqueous dynamics. Exp Eye Res 2004; 78:633-7. [PMID: 15106943].

29. Hirt J, Liton PB. Autophagy and mechanotransduction in outflow pathway cells. Exp Eye Res 2017; 158:146-53. [PMID: 27373974].

30. Morozumi W, Inagaki S, Iwata Y, Nakamura S, Hara H, Shimazawa M. Piezo channel plays a part in retinal ganglion cell damage. Exp Eye Res 2020; 191:107900-[PMID: 31874142].

31. Read AT, Chan DW, Ethier CR. Actin structure in the outflow tract of normal and glaucomatous eyes. Exp Eye Res 2007; 84:214-26. [PMID: 17219625].

32. Sherwood ME, Richardson TM. Phagocytosis by trabecular meshwork cells: sequence of events in cats and monkeys. Exp Eye Res 1988; 46:881-95. [PMID: 3197758].

33. Stamer WD, Braakman ST, Zhou EH, Ethier CR, Fredberg JJ, Overby DR, Johnson M. Biomechanics of Schlemm's canal endothelium and intraocular pressure reduction. Prog Retin Eye Res 2015; 44:86-98. [PMID: 25223880].

34. Braakman ST, Pedrigi RM, Read AT, Smith JA, Stamer WD, Ethier CR, Overby DR. Biomechanical strain as a trigger for pore formation in Schlemm's canal endothelial cells. Exp Eye Res 2014; 127:224-35. [PMID: 25128579].

35. Bagriantsev SN, Gracheva EO, Gallagher PG. Piezo proteins: regulators of mechanosensation and other cellular processes. J Biol Chem 2014; 289:31673-81. [PMID: 25305018].

36. Alm A, Nilsson SF. Uveoscleral outflow–a review. Exp Eye Res 2009; 88:760-8. [PMID: 19150349].

37. McMillin MJ, Beck AE, Chong JX, Shively KM, Buckingham KJ, Gildersleeve HI, Aracena MI, Aylsworth AS, Bitoun P, Carey JC, Clericuzio CL, Crow YJ, Curry CJ, Devriendt K, Everman DB, Fryer A, Gibson K, Giovannucci Uzielli ML, Graham JM Jr, Hall JG, Hecht JT, Heidenreich RA, Hurst JA, Irani S, Krapels IP, Leroy JG, Mowat D, Plant GT, Robertson SP, Schorry EK, Scott RH, Seaver LH, Sherr E, Splitt M, Stewart H, Stumpel C, Temel SG, Weaver DD, Whiteford M, Williams MS, Tabor HK, Smith JD, Shendure J, Nickerson DA, Bamshad MJ. Mutations in PIEZO2 cause Gordon syndrome, Marden-Walker syndrome, and distal arthrogryposis type 5. Am J Hum Genet 2014; 94:734-44. [PMID: 24726473].

38. Coste B, Houge G, Murray MF, Stitziel N, Bandell M, Giovanni MA, Philippakis A, Hoischen A, Riemer G, Steen U, Steen VM, Mathur J, Cox J, Lebo M, Rehm H, Weiss ST, Wood JN, Maas RL, Sunyaev SR, Patapoutian A. Gain-of-function mutations in the mechanically activated ion channel PIEZO2 cause a subtype of Distal Arthrogryposis. Proc Natl Acad Sci USA 2013; 110:4667-72. [PMID: 23487782].

39. Haliloglu G, Becker K, Temucin C, Talim B, Kucuksahin N, Pergande M, Motameny S, Nurnberg P, Aydingoz U, Topaloglu H, Cirak S. Recessive PIEZO2 stop mutation causes distal arthrogryposis with distal muscle weakness, scoliosis and proprioception defects. J Hum Genet 2017; 62:497-501. [PMID: 27974811].

40. Alcaino C, Farrugia G, Beyder A. Mechanosensitive Piezo Channels in the Gastrointestinal Tract. Curr Top Membr 2017; 79:219-44. [PMID: 28728818].

41. Alcaino C, Knutson KR, Treichel AJ, Yildiz G, Strege PR, Linden DR, Li JH, Leiter AB, Szurszewski JH, Farrugia G, Beyder A. A population of gut epithelial enterochromaffin cells is mechanosensitive and requires Piezo2 to convert force into serotonin release. Proc Natl Acad Sci USA 2018; 115:E7632-41. [PMID: 30037999].

42. Koser DE, Thompson AJ, Foster SK, Dwivedy A, Pillai EK, Sheridan GK, Svoboda H, Viana M, Costa LD, Guck J, Holt CE, Franze K. Mechanosensing is critical for axon growth in the developing brain. Nat Neurosci 2016; 19:1592-8. [PMID: 27643431].

Articles are provided courtesy of Emory University and the Zhongshan Ophthalmic Center, Sun Yat-sen University, P.R. China. The print version of this article was created on 20 May 2021. This reflects all typographical corrections and errata to the article through that date. Details of any changes may be found in the online version of the article.